Galaxea, Journal of Coral Reef Studies 16: 1−10 (2014)

Original paper

Calcification, photosynthesis and nutritional status of the hermatypic coral *Porites lutea*: contrasting case studies from Indonesia and Thailand

Yvonne SAWALL[1,*], Somkiat KHOKIATTIWONG[2], Jamaluddin JOMPA[3], and Claudio RICHTER[4]

[1] Leibniz Center for Tropical Marine Ecology, 28359 Bremen, Germany
[2] Phuket Marine Biological Center, Phuket 83000, Thailand
[3] Center for Coral Reef Research, Hasanuddin University, Makassar 90245, Indonesia
[4] Alfred Wegener Institute, Helmholtz Center for Polar and Marine Research, 27568 Bremerhaven, Germany
* Current address: Helmholtz Center for Ocean Research, 24148 Kiel, Germany

* Corresponding author:
E-mail: ysawall@geomar.de

Communicated by Beatriz E. CASARETO (Biogeochemistry Editor)

Abstract *In situ* incubation experiments, complemented by tissue analyses, were conducted with the coral *Porites lutea* at four sites featuring contrasting environmental conditions: two shallow (3 m) reefs in Spermonde Archipelago (Indonesia) subjected to coastal pollution (Lae Lae, *LL*) and oligotrophic waters (Bonebatang, *BBA*), respectively; a deep (20 m, *KR-D*) and a shallow (7 m, *KR-S*) reef at off-shore Ko Racha (KR) in the Andaman Sea (Thailand) subjected to pulsed upwelling. Mean temperature varied only little (29−30℃). While most tissue parameters responded to light and nutrient changes as expected, metabolic rates revealed surprising patterns: 3-fold elevated calcification occurred at *KR-S* compared to all other sites despite reduced gross photosynthesis. Furthermore, equal photosynthesis occurred in 7 and 20 m depth at KR, despite a 5-fold reduction in light intensity, which could not be solely ascribed to photo-acclimation processes, such as increased cell-specific chlorophyll *a* in 20 m depth. These findings support the notion of a highly flexible species and indicate that this might partly be ascribed to a strong variation in the internal turnover of oxygen and nutrients between coral host and zooxanthellae, meaning a strong variation in the rates of energy acquisition. Those differences are particularly difficult to determine *in situ*, but require greater attention in the future in order to enhance our understanding of metabolic processes and acclimatization abilities.

Keywords metabolic plasticity, *Porites lutea*, eutrophication, pulsed upwelling, calcification, photosynthesis, internal turnover

Introduction

One of the most wide-ranging hermatypic coral species is *Porites lutea* (Edwards and Haime, 1851), which is found from the Red Sea across the Indian and Pacific Ocean to the western shores of Mexico. It thrives in oligotrophic, in turbid backreef and in coastal environments subjected to runoff of sediments and nutrients from land

(Scoffin et al. 1992; Veron 2000). This hints at a high phenotypic plasticity and/or at genetic adaptations of the coral host and/or their symbionts, the zooxanthellae. Various factors are known to influence the coral host and zooxanthellae, which have been assessed under controlled conditions in aquaria or in regionally restricted areas (e.g. depth gradient, eutrophication gradient). Examples are: (i) Decreasing light increases chlorophyll *a* (chl *a*) in zooxanthellae (Dubinsky et al. 1990; Titlyanov et al. 2001). (ii) Increasing nutrients (organic) increase heterotrophy hence coral biomass and zooxanthellae density, which lead to increased photosynthesis and potentially also to increased calcification (Fabricius 2005; Houlbrèque and Ferrier-Pages 2008). Feeding capacity, however, is highly variable between symbiotic corals where the symbionts usually provide the majority of energy through photosynthesis (Anthony and Connolly 2004; Grottoli et al. 2006). (iii) Increasing particle loads increase mucus production, meaning a higher loss of energy and carbon through mucus release (Edmunds and Davies 1989). (iv) high light / photosynthesis supports calcification inter alia by the provision of fast energy (Tambutté et al. 2011). So far, physiological studies on reef corals of south-east Asia are scarce, and *in situ* studies across regions are lacking.

Here, we assessed the physiological characteristics (metabolic rates and tissue parameters) of *P. lutea* from contrasting environmental conditions in terms of nutrient regimes, light intensity, and exposure, however within a very narrow temperature regime (29−30℃). The aim of the study was to investigate the coral's phenotypic plasticity and to validate generally accepted dependencies between environmental and physiological responses in two environmentally contrasting regions, in the Andaman Sea of Thailand and in the Spermonde Archipelago of Indonesia.

Material and Methods

Field experiments were carried out at four reef sites; two sites in Spermonde Archipelago, Sulawesi, Indonesia and two sites at Ko Racha, Andaman Sea, Thailand. In Spermonde, untreated effluents of the major harbour city Makassar and land-run off from aqua- and agriculture create a strong cross-shelf gradient in water quality (Edinger et al. 1998; Renema and Troelstra, 2001). The near-shore turbid and polluted reef Lae Lae (*LL*, 2 km distance to shore) and the oligotrophic mid-shelf reef Bonebatang (*BBA*, 12 km distance to shore) were selected to present opposite sides of the cross-shelf gradient (Fig. 1, Tab. 1). Maximum reef depth at *LL* was 5 m, hence experiments were carried out at 3 m depth near the reef edge at both sites. Ko Racha (KR) is an exposed island 11 km south of Phuket in the Andaman Sea close to the continental shelf edge featuring oceanic water conditions (Scoffin et al. 1992). Here, monsoonal waves and large amplitude internal waves (LAIW) induced pulsed upwelling of cold, nutrient-rich, low pH and oxygen-depleted water (Osborne and Burch 1980; Roder et al. 2010, Tab. 1), which constrain coral growth to a band of 7 to 25 m. One shallow (7 m, *KR-S*) and one deep (20 m, *KR-D*) site were chosen on the western side of KR (Fig. 1), where coral collection and experiments were performed. The experiments were conducted in October and November 2008 in Spermonde and in March 2009 at KR. Due to the orography in south-east Asia, the timing of the monsoon varies significantly between regions and the timing of our study corresponds to the end of the dry season in both regions.

Fragments of *P. lutea* were chiselled off the upper side of the colonies (one fragment per colony). They were prepared and incubated *in situ* in the corresponding depths as described elsewhere (Sawall et al. 2011). At KR sites, 5 light (photosynthesis [P], light calcification [G_L]) and 5 dark (respiration [R], dark calcification [G_D]) coral incubations, as well as 3 light and 3 dark coral-free control incubations were repeated over 3 consecutive days, yielding a total of 15 (9) coral (control) replicates each for *KR-S* and *KR-D*. In Spermonde, 2 light and 2 dark coral incubations and 2 light and 2 dark coral-free control incubations were repeated over 3 consecutive days, yielding 6 replicates for both, corals and coral-free controls, in *LL* and *BBA* (decreased chamber number due to technical reasons). Incubations started at maximum irradiance (1:00 pm local time) and lasted for 1 to 1.5 hrs. Net P (P_n), gross P (P_g) and R were determined by measuring the oxygen concentration in the beginning and at the end of the incubations. G_L and G_D were determined via the alkalinity

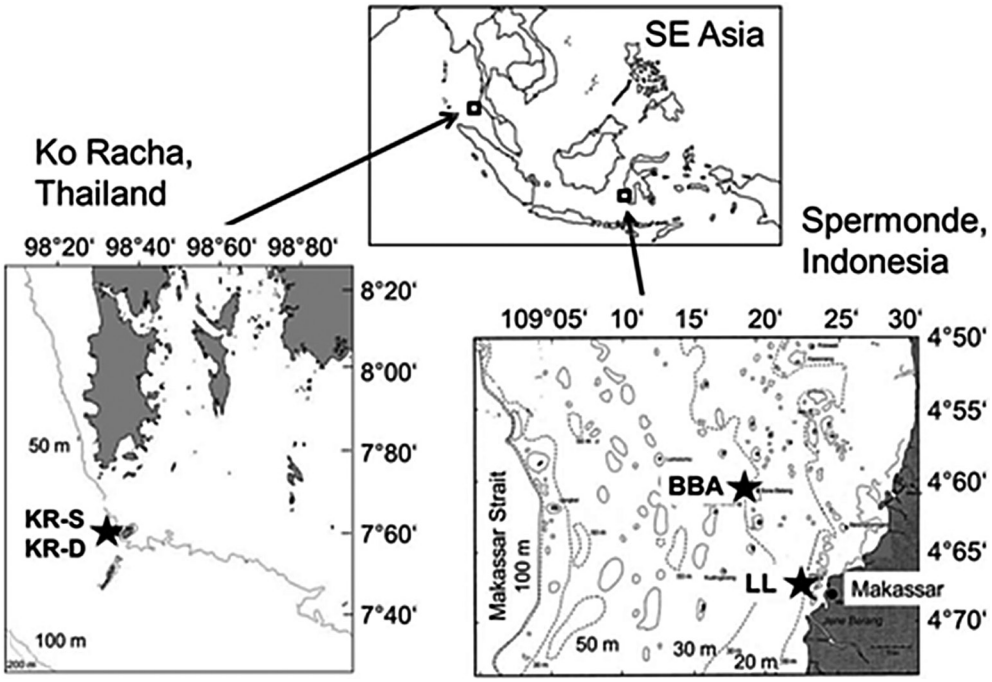

Fig. 1 Locations of study sites in front of the island Ko Racha (KR-S and KR-D) and in Spermonde Archipelago (Bonebatang, BBA and Lae Lae, LL).

Table 1 Water parameter at the sites Bonebatang (BBA) and Lae Lae (LL) in Spermonde Archipelago and at the sites Ko Racha shallow (KR-S) and Ko-Racha deep (KR-D) at the off-shore island Ko Racha. Total suspended solids (TSS), chlorophyll *a* (chl *a*), particulate organic carbon (POC), particulate organic matter (POM), dissolved organic carbon (DOC), photosynthetic active radiation in the corresponding depth measured during experiment (PAR_{depth}(measured)) and derived from NASA (monthly averaged surface values allocated with K_d values – PAR_{depth}(NASA) . Values given as mean (standard error). Samples and measurements taken during incubations. Analyses done after standard procedures (see Supplementary Information). No data (n.d.).

	Spermonde		Ko Racha	
	BBA	LL	KR-S	KR-D
Depth [m]	3	3	7	20
Turbidity [K_d]	-0.17 (<0.01)	-0.30 (<0.01)	-0.21 (<0.01)	-0.17 (<0.01)
TSS [mg l^{-1}]	1.98 (0.61)	6.93 (1.53)	5.05 (0.31)	7.17 (0.41)
Chl a [µg l^{-1}]	0.36 (0.03)	0.71 (0.05)	0.51 (0.10)	0.39 (0.03)
POC [µg l^{-1}]	104.7 (11.8)	236.2 (22.8)	133.3 (13.9)	143.3 (9.5)
C/N ratio POM	9.57 (1.65)	7.83 (1.02)	7.98 (0.94)	9.18 (1.00)
DOC [µM]	52.2 (7.1)	61.7 (0.8)	209.4 (30.7)	306.3 (88.1)
PAR_{depth} (measured) [µE m^{-2} s^{-1}]	596 (93)	611 (103)	329 (11)	61 (2)
PAR_{depth} (NASA) [E m^{-2} day^{-1}]	28.04	18.99	10.99	1.60
Temperature [°C]	29.41 (0.01)	29.95 (0.01)	n.d.	28.77 (0.01)
pH	8.40 (<0.01)	8.38 (<0.01)	n.d.	8.14 (<0.01)
Current velocity [m s^{-1}]	0.045 (0.001)	0.035 (0.001)	n.d.	0.104 (0.002)

anomaly method (Schneider and Erez 2006; Sawall et al. 2011). Light measurements were taken between 1:00 and 2:00 pm with an underwater light meter (LiCor Li-192SA, Lincoln, USA) during incubations in the corresponding depth, measuring photosynthetic active radiation (PAR, µmol photons m^{-2} s^{-1}).

Tissue extraction, processing, and analyses were conducted as described by Sawall et al. (2011). Shortly, after incubation tissue was removed from the skeleton with an air gun and 0.7 µm filtered seawater. The tissue slurry was homogenized and sub-samples were stored at −20℃ until analysis. Zooxanthellae density was determined with a haemocytometer (Fuchs-Rosenthal chamber) under the light microscope, chl *a* was measured fluorometrically after extraction with acetone, dry biomass of the tissue was determined gravimetrically. Protein concentration was measured with a photometer after Bradford (1976) in host tissue and zooxanthellae after separation by centrifugation and sonication for cell wall break down. The surface area of the coral fragments was determined gravimetrically using the wax coating technique (Naumann et al. 2009). Replication size of the tissue parameter were double the amount of the metabolic rates, since each coral fragment was either used for light or for dark incubation, while tissue analyses were conducted for all fragments.

Metabolism and tissue data were tested for normal distribution and transformed, where necessary. One-way ANOVA and post-hoc Tukey for unequal sample size were applied to assess differences between the sites (Statistica 9). Multivariate statistics (Primer v6, PERMANOVA) were applied to explore trends and dependencies between the different biological and environmental variables (Clarke and Gorley 2006). For this, a redundancy analysis, step-wise forward (named DistLM in Primer), was performed with the environmental data set (Tab. 1) as the predictor variables, (Euclidean distance) and the two biological data sets, metabolic parameters and tissue parameters, as the response variables (Bray-Curtis similarity). The applied environmental data sets for the two separate DistLM tests were the same, although with one exception: PAR_{depth} (measured) was included only for testing potential effects on metabolic rates and PAR_{depth} (NASA) was included only for testing potential effects on tissue parameters.

Results

P_g was about 65 % higher in eutrophic *LL* compared to oligotrophic *BBA* (Fig. 2a) in spite of similar average PAR intensities of around 600 µmol photons m^{-2} s^{-1} during incubations (PAR_{depth} [measured], Tab. 1). At KR, P_g was similar in shallow and deep (Fig. 2a) in spite of 5-fold differences in measured light intensity (Tab. 1). This pattern was consistent for KR, if P_g was standardized to areal chl *a* (Tab. S1). In contrast, G_L of *P. lutea* were similar at *BBA* and *LL* but almost 3-fold higher in *KR-S* compared to all other sites (Fig. 2b). Although, this pattern was reduced when G_L was standardized to biomass (1.5−2-fold difference between *KR-S* and Spermonde reefs) the difference remained the same between *KR-S* and *KR-D* (Tab. S1). The G_L/G_D ratios were more than 2-fold higher at KR, compared to Spermonde (Tab. S1).

Zooxanthellae densities were almost 75 % higher in *LL*

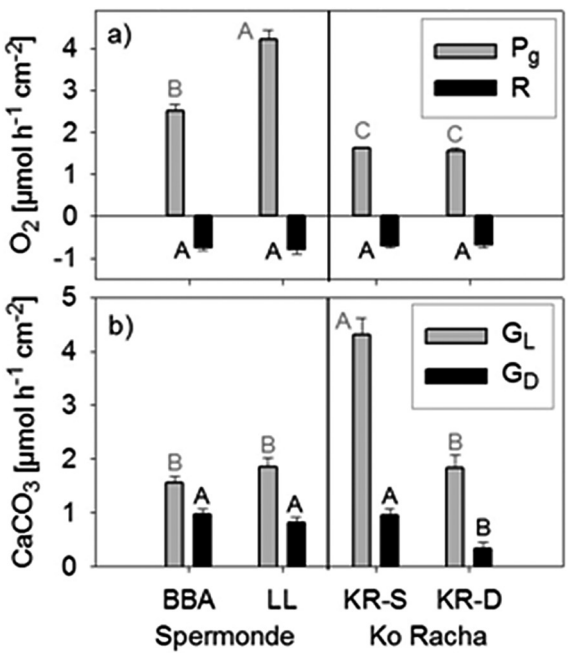

Fig. 2 Metabolism of the coral holobiont. **a**) Gross photosynthesis (P_g) and respiration (R). **b**) Light calcification (G_L) and dark calcification (G_D). Bars represent mean ± SE (BBA and LL: n = 6; KR-S and KR-D: n = 15). Significant differences ($p < 0.05$) are indicated by capital letters.

than in *BBA*, while in KR they were similar in shallow and deep, being between the densities found at *LL* and *BBA* (Fig. 3a) The cell-specific chl *a* concentrations were comparatively low and similar in *LL* and *BBA*, while they were around 3-fold higher in KR and particularly high at *KR-D* (Fig. 3a). The cell-specific protein contents (ZProt) of *LL* and *KR-D* corals (~0.3−0.4 ng zooxanthellae^{-1}) were about half the concentrations of the *BBA* and *KR-S* corals (Tab. S1). The coral tissue biomass increased consecutively from *BBA* to *LL*, *KR-S* and *KR-D,* while the absolute increase was more than 2-fold (Fig. 3b). The protein content of the biomass (% TProt) was particularly high at *KR-S,* being about 1.5-fold higher than at all other sites (Fig. 3b). All values of biological data (mean±SE) are available as Supplementary Information in table S1.

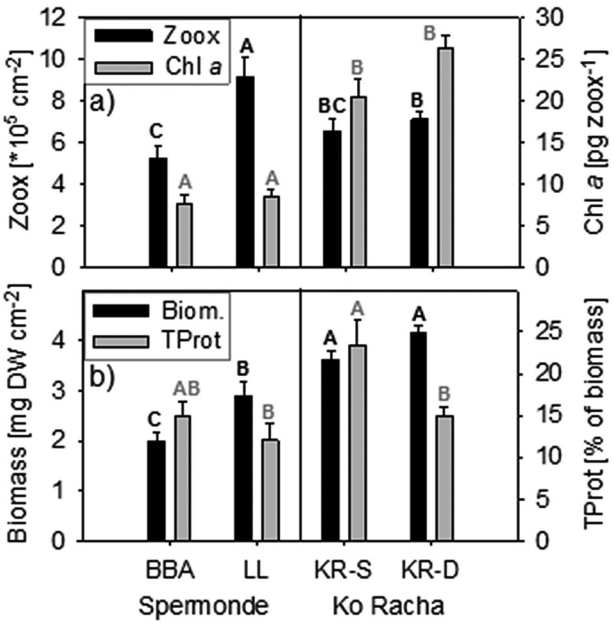

Fig. 3 Tissue parameter of the coral holobiont. **a**) Zooxanthellae (zoox) density and chlorophyll *a* (chl *a*) per zooxanthellae. **b**) Biomass (biom.) in mg dry weight (DW) and animal tissue protein (TProt). Bars represent mean ±SE (BBA and LL: n=12; KR-S and KR-D: n=30). Significant differences ($p<0.5$) are indicated by capital letters.

The pattern of the metabolism rates was best explained by the environmental parameter DOC, followed by the C/N ratio of POM and the turbidity with a cumulative probability of 50.8% (Tab. 2). The pattern of the tissue parameter could be explained best by PAR_{depth} (NASA), followed by TSS and turbidity resulting in a cumulative probability of 35.8% (Tab. 2).

Discussion

The contrasting environmental settings of light intensity and nutrient related environmental parameters revealed significant effects on the tissue composition and metabolic rates, however not always as expected. The most remarkable results were (i) 3-fold higher G_L rate in *KR-S* compared to all other sites despite a low P_g rate and (ii) equal

Table 2 DistLM results. The upper part of the table presents the probable effects of environmental parameters on the metabolic rates and the lower part the probable effects on the tissue parameters. Cumulative probability (Cumul. prob.).

Response variables: metabolic measurements					
	Adjusted R^2	Sum of squares	Pseudo-F	p	Cumul. prob. [%]
DOC	0.337	13198	36.5	0.001	34.6
C/N ratio of POM	0.439	4162	13.6	0.001	45.5
Turbidity	0.486	2012	7.2	0.002	50.8
PAR_{depth} (measured)	0.493	546	2.0	0.094	52.2
Response variables: tissue parameters					
PAR_{depth} (NASA)	0.239	9687	23.0	0.001	25.0
TSS	0.295	2522	6.5	0.002	31.5
Turbidity	0.329	1663	4.5	0.009	35.8
DOC	0.332	498	1.3	0.272	37.1

P_g rates at *KR-S* and *KR-D* despite a 5-fold difference in light intensity.

Photosynthesis is the main energy source for the coral holobiont (Muscatine et al. 1984; Dubinsky and Jokiel 1994), and the two most important parameters influencing zooxanthellae performance, hence photosynthesis, are nutrient and light availability (Dubinsky et al. 1990; Titlyanov et al. 2001). A clear effect of the monthly averaged PAR intensities on zooxanthellae composition was evident, explaining increasing pigmentation (chl *a* per zooxanthellae) from high light *BBA* to low light *KR-D* (Titlyanov et al. 2001). Nutrient-related parameters (e.g. TSS and turbidity) explain increased zooxanthellae densities (Houlbrèque and Ferrier-Pagès 2008; Fabricius 2005) in near-shore *LL* compared to off-shore *BBA* and medium values at the two KR sites. Furthermore, increased zooxanthellae densities explain the strongly elevated P_g rates at *LL* compared to *BBA*, which occurred despite similar light intensities during incubations (PAR_{depth} [measured]; turbidity was lower in *BBA*, but cloudiness was higher during incubations). However, comparing now KR reefs with Spermonde reefs, it seems that the strongly increased cell-specific chl *a* concentrations at KR reefs (photo-acclimation) concomitant with intermediate zooxanthellae densities were not able to counterbalance reduced light intensities with regard to photosynthesis. In particular at *KR-S*, photosynthetic rates seem to be very low, considering firstly that the zooxanthellae were well-equipped (high chl *a* and protein content) and secondly that the light intensity varied greatly between *KR-S* and *KR-D* (5-fold). On top of this, *KR-S* featured by far the highest day calcification rates, which do not match the low P_g rates and will be discussed later (second next paragraph).

The relative contribution of heterotrophy to the coral's nutrition under decreasing light intensity and/or increasing food availability is dependent on the corals trophic plasticity (e.g. Anthony & Connolly 2004). Increased heterotrophy seems to be the case at KR if compared to Spermonde, indicated by higher biomass values as well as by elevated protein concentration in the animal tissue and zooxanthellae (Houlbrèque and Ferrier-Pagès 2008) at KR. However, TSS concentrations were similar at the KR reefs and eutrophied *LL* and POM was even higher at *LL*, which would infer equally or higher biomass and protein levels in *LL*. This promotes the idea that the DOC concentrations largely determine heterotrophic rates, which were in average 5-fold higher (DOC) at the KR sites compared to the Spermonde reefs. DOC contains inter alia free amino acids and microorganisms, which were shown to be taken up by some corals in substantial amounts (reviewed by Houlbrèque and Ferrier-Pagès 2008), and which may even be the preferred food source for small-polyped corals like *P. lutea*. The uptake of DOC may additionally feed the bacterial activity within the coral's gastric cavity, which would fuel nutrient turnover and availability, and consequently increase the coral's metabolism (Agostini et al. 2012). Increased metabolism, particularly at *KR-S,* is also supported by the high calcification rates.

Hence, various parameters indicate that *KR-S* corals are well-functioning and highly active, which suggests that the P_g rates are considerably underestimated at that site. Similar photosynthetic rates of corals under very different natural light regimes (depth gradient) were previously found and associated to differences in light respiration rates (Titlyanov et al. 1991), including the coral *P. lutea* (Jantzen et al. 2013). This is supported by earlier respirometer studies, which showed post-illumination enhanced respiration (PIER) by the coral host in response to increased supplies of O_2 and photosynthates by the photosynthetic symbionts (Edmund and Davies 1988). Furthermore, microsensor studies revealed even higher (up to 11-fold) respiration rates within the first few seconds after switching off the light (Al-Horani et al. 2003), suggesting that respiration rates are much higher in the light than in the dark (Nakamura et al. 2013). This means also that the internal turnover and hence the supply of energy is much higher than what we derive from classical respirometer studies, and that they may vary substantially under different environmental conditions (not only concerning light availability but also for example exposure, nutrients, temperature). Although it is difficult to determine these turnover rates, particularly in the field, we have strong support that differences in turnover rates occurred in our study. The following mechanism is suggested, explaining the strong underestimation of the calculated P_g particularly at *KR-S*: 1. increased heterotrophy of DOC increases

biomass and nutrient availability (if compared to Spermonde), 2. increased nutrient availability together with reduced light levels increases cell-specific chl *a* of the zooxanthellae (if compared to Spermonde), 3. increased nutrient availability together with better facilitated zooxanthellae increase autotrophy, 4. increased autotrophy increases oxygen and energy supply to the coral host, 5. this increases the metabolic activity of the coral host which pushes the internal turnover (recycling of O_2 and nutrients), 6. high internal turnover results in high energy supply, which supports (inter alia) high G_L rates (Nakamura et al. 2013). Those might be necessary to grow in the harsh LAIW-controlled environment at KR. At night (dark), calcification rates are strongly reduces at both KR sites (G_L/G_D rates >4.5) highlighting again the comparatively high activity of KR corals during the day, particularly at *KR-S*.

In Spermonde, similar G_L rates at both sites, despite substantially increased P_g rates at the eutrophic site *LL,* indicates an allocation of surplus energy / carbon at *LL* into other processes than G_L. Promoted processes at *LL* certainly include zooxanthellae growth (increased densities) (Edmunds and Davies 1989; Muscatine et al. 1989), but most likely also mucus production, which is usually higher in turbid waters (Crossland 1987; Anthony and Connolly 2004), thus preventing smothering by sediments (Edmunds and Davies 1989). Similar observations were made also for the coral *Stylophora subseriata* in Spermonde (Sawall et al. 2011).

In conclusion, the large differences in energy acquisition and allocation encountered in our case studies support the notion of a highly flexible species able to cope with various conditions. However, it also demonstrates the complexity of metabolic responses to environmental conditions, which might not only be ascribed to the metabolic plasticity but also to genotypic variability. In order to improve our understanding about acclimatization / adaptation processes of corals studies on their metabolism need to be intensified into the direction of the assessment of internal processes. Furthermore, they require a sophisticated monitoring of environmental parameters and longer-term metabolism studies in order to discriminate between more and less important environmental drivers and they need to be combined with genetic analyses.

Acknowledgments

We thank the directors and staff of UNHAS, PMBC, ZMT and AWI for their support in the organization and execution of the field work and for providing assistance, material and laboratory space. Thanks are due to N. Phongsuwan for species verification. This study was funded by the German Federal Ministry of Education and Research (BMBF) under the bilateral German-Indonesian project (SPICE) [grant number 03F0472A] with support from German Research Foundation (DFG) [grant number RI 1074/7-1].

References

Agostini S, Suzuki Y, Higuchi T, Casareto BE, Yoshinaga K, Nakano Y, Fujimura H (2012) Biological and chemical characteristics of the coral gastric cavity. Coral Reefs 31: 147−156

Al-Horani FA, Al-Moghrabi SM, de Beer D (2003) The mechanism of calcification and its relation to photosynthesis and respiration in the scleractinian coral *Galaxea fascicularis*. Mar Biol 142: 419−426

Allemand D, Tambutté E, Girard JP, Jaubert J (1998) Organic matrix synthesis in the scleractinian coral stylophora pistillata: role in biomineralization and potential target of the organotin tributyltin. J Exp Biol 201: 2001−2009

Anthony KRN, Connolly SR (2004) Environmental limits to growth: physiological niche boundaries of corals along turbidity-light gradients. Oecologia 141: 373−384

Bradford M (1976) A rapid and sensitive method for the quantitation of microgram quantities of protein utilizing the principle of protein-dye binding. Anal Biochem 72: 248−254

Clarke KR, Gorley RN (2006) PRIMER v6: User manual / tutorial, Vol. PRIMER-E Ltd, Plymouth, England

Crossland CJ (1987) In situ release of mucus and DOC-lipid from the corals *Acropora variabilis* and *Stylophora pistillata* in different light regimes. Coral Reefs 6: 35−42

Dubinsky Z, Jokiel PL (1994) Ratio of energy and nutrient fluxes regulates symbiosis between zooxanthellae and corals. Pac Sci 48: 313−324

Dubinsky Z, Stambler N, Ben-Zion M, McCloskey LR, Muscatine L, Falkowski PG (1990) The effect of external

nutrient resources on the optical properties and photosynthetic efficiency of *Stylophora pistillata*. Proc R Soc Lond, B 239: 231−246

Edinger EN, Jompa J, Limmon GV, Widjatmoko W, Risk MJ (1998) Reef degradation and coral biodiversity in Indonesia: Effects of land-based pollution, destructive fishing practices and changes over time. Mar Pollut Bull 36: 617−630

Edmunds PJ, Davies PS (1988) Post-illumination stimulation of respiration rate in the coral *Porites porites*. Coral Reefs 7: 7−9

Edmunds PJ, Davies PS (1989) An energy budget for *Porites porites* (Scleractinia), growing in a stressed environment. Coral Reefs 8: 37−43

Fabricius KE (2005) Effects of terrestrial runoff on the ecology of corals and coral reefs: review and synthesis. Mar Pollut Bull 50: 125−146

Grottoli AG, Rodrigues LJ, Palardy JE (2006) Heterotrophic plasticity and resilience in bleached corals. Nature 440: 1186−1189

Houlbrèque F, Ferrier-Pagès C (2008) Heterotrophy in tropical scleractinian corals. Biol Rev 84: 1−17

Jantzen C, Schmidt GM, Wild C, Roder C, Khokiattiwong S, Richter C (2013) Benthic Reef Primary Production in Response to Large Amplitude Internal Waves at the Similan Islands (Andaman Sea, Thailand). PLoS ONE 8: e81834

Muscatine L, Falkowski PG, Dubinsky Z, Cook PA, McCloskey LR (1989) The effect of external nutrient resources on the population dynamics of zooxanthellae in a reef coral. Proc R Soc Lond B 236: 311−324

Muscatine L, Falkowski PG, Porter JW, Dubinsky Z (1984) Fate of photosynthetic fixed carbon in light- and shade-adapted colonies of the symbiotic coral *Stylophora pistillata*. Proc R Soc Lond B 222: 181−202

Nakamura T, Nadaoka K, Watanabe A (2013) A coral polyp model of photosynthesis, respiration and calcification incorporating a transcellular ion transport mechanism. Coral Reefs 32: 779−794

Naumann MS, Niggl W, Laforsch C, Glaser C, Wild C (2009) Coral surface area quantification-evaluation of established techniques by comparison with computer tomography. Coral Reefs 28: 109−117

Osborne AR, Burch TL (1980) Internal solitons in the Andaman Sea. Science 208: 451−460

Renema W, Troelstra SR (2001) Larger foraminifera distribution on a mesotrophic carbonate shelf in SW Sulawesi (Indonesia). Palaeogeogr Palaeoclimatol Palaeoecol 175: 125−146

Roder C, Fillinger L, Jantzen C, Schmidt G, Khokiattiwong S, Richter C (2010) Trophic response of corals to large amplitudal internal waves. Mar Ecol Prog Ser 412: 113−128

Sawall Y, Teichberg MC, Seemann J, Litaay M, Jompa J, Richter C (2011) Nutritional status and metabolism of the coral *Stylophora subseriata* along a eutrophication gradient in Spermonde Archipelago (Indonesia). Coral Reefs 30: 841−853

Schneider K, Erez J (2006) The effect of carbonate chemistry on calcification and photosynthesis in the hermatypic coral *Acropora eurystoma*. Limnol Oceanogr 51: 1284−1293

Scoffin TP, Tudhope AW, Brown BE, Chansang H, Cheeney RF (1992) Patterns and possible environmental controls of skeletogenesis of *Porites lutea*, South Thailand. Coral Reefs 11: 1−11

Tambutté S, Holcomb M, Ferrier-Pagès C, Reynaud S, Tambutté É, Zoccola D, Allemand D (2011) Coral biomineralization: From the gene to the environment. J Exp Mar Biol Ecol 408: 58−78

Titlyanov EA (1991) The stable level of coral primary production in a wide light range. In: Williams RB, Cornelius PFS, Hughes RG, Robson EA (eds) Coelenterate Biology: Recent Research on Cnidaria and Ctenophora. Springer Netherlands, pp 383−387

Titlyanov EA, Titlyanova TV, Yamazato K, van Woesik R (2001) Photo-acclimation of the hermatypic coral *Stylophora pistillata* while subjected to either starvation or food provisioning. J Exp Mar Biol Ecol 257: 163−181

Veron JEN (2000) Corals of the world. Australian Institute of Marine Science and CRR Qld Pty Ltd, Townsville

Received: 23 May 2013
Accepted: 3 April 2014

Supplementary

Environmental data collection during the experiments

Light intensity profiles were taken between 1:00 and 2:00 pm with an underwater light meter (LiCor Li-192SA, Lincoln, USA) on the experimental days (3 per site), measuring the photosynthetic active radiation (PAR, µmol photons m^{-2} s^{-1}) just above and below the surface and

every 0.5 m down to 6 m depth. The light attenuation coefficient (K_d) was calculated as a measure of turbidity after Dennison et al. (1993) for each site using the equation $E(z)=E_o \times e^{-K_d \times z}$, where E_o and E(z) are the light intensities (PAR) just below the surface and in 6 m depth, respectively, and z is the difference in depth (6 m).

Triplicate water samples were taken at all sites and depths with a 5-l Niskin bottle. From each water sample, one 1-l sub sample was filtered on a GF/F filter to determine the chlorophyll *a* (chl *a*) concentration, three 1-l subsamples were filtered on three pre-combusted and pre-weighed GF/F filter, for analyses of total carbon (C_{tot}) and nitrogen (N_{tot}) and organic carbon (POC) of the particulate organic matter (POM). Filters were stored at −20℃. A 10-ml sample from the filtrate was filled into a glass ampoule, acidified with H_3PO_4 (pH <2.0) and flame sealed for dissolved organic carbon (DOC) analyses. Chl *a* was extracted from the defrosted filter with 90% acetone over 24 h at 4℃, the sample was centrifuged (4000 rcf, 5 min) and measured fluorometrically (10-AU Fluorometer, Turner Design, CA) in a glass cuvette at an emission wavelength of 668 nm and an excitation wave length of 430 nm (Boto and Bunt, 1978). Calibration was carried out with a chl *a* standard (Fluka, Sigma-Aldrich, Switzerland). Filters for C_{tot}, N_{tot} and POC analyses were dried, the weight of total suspended solids (TSS) determined and the concentrations of the elements were measured with an elemental analyzer (NA2100 Protein, calibrated with CHNS standard [LECO]). Filters for POC analyses were acidified with 1 N HCl and dried prior to analysis to remove the inorganic carbon. DOC was measured via the combustion method with a total organic carbon analyzer (TOC-V_{CPH}, Shimadzu) using low carbon and deep sea water standards (Hansell, RSMAS, Univ. of Miami).

In order to evaluate the potential effect of the average light intensity, the monthly average products of photosynthetic active radiation (PAR) were derived from satellite images from NASA, Giovanni Ocean Color Radiometry, data set from MODIS aqua 4 km, available online. These values correspond to PAR at the surface in October 2008 for Spermonde and in March 2009 for Ko Racha, which were used to calculate PAR in the corresponding depth (PAR_{depth} (NASA)) using K_d and the equation descried above.

Current velocity was measured with an Acoustic Doppler Current Profiler (1200 kHz Workhorse Sentinel ADCP, Teledyne RD Instruments) deployed at 4 m (Spermonde) and 20 m (Ko Racha) near the incubation sites, with a bin size of 1 m. The bins corresponding to the depths of experiments were analyzed. Temperature loggers (Tidbit v2 Temp, Bourne, MA, USA) were deployed at 10 and 20 m depth in Ko Racha in order to confirm the occurrence of LAIW.

References

Boto KG, Bunt JS (1978) Selective excitation fluorometry for the determination of chlorophylls and pheophytins. Analytical Chemistry 50: 392−395

Dennison WC, Orth RJ, Moore KA, Stevenson JC, Carter V, Kollar S, Bergstrom PW, Batiuk RA (1993) Assessing water quality with submersed aquatic vegetation. BioScience 43: 86−94

Table S1 Metabolic rates and tissue composition. Metabolic rates Spermonde n=6, Ko Racha n=15; tissue parameter Spermonde n=12, Ko Racha n=30. Mean (±SE). Gross photosynthesis (P_g), respiration (R), light (G_L) and dark calcification (G_D), zooxanthellae (zoox), chlorophyll *a* (chl *a*), zooxanthellar protein (ZProt), host tissue protein (TProt), biomass (biom.).

	Spermonde		Ko Racha	
	BBA	LL	KR-S	KR-D
P_g cm^{-2} [µmol O_2 h^{-1}]	2.52 (0.13)	4.22 (0.22)	1.63 (0.01)	1.56 (0.06)
P_g zoox^{-1} [pg O_2 h^{-1}]	5.25 (0.52)	5.07 (0.52)	2.99 (0.24)	2.47 (0.17)
P_g µg^{-1} chl *a* [µmol O_2 h^{-1}]	0.74 (0.07)	0.61 (0.05)	0.17 (0.02)	0.1 (0.01)
R cm^{-2} [µmol O_2 h^{-1}]	0.75 (0.05)	0.79 (0.11)	0.7 (0.05)	0.69 (0.06)
R mg^{-1} biom. [µmol O_2 h^{-1}]	0.38 (0.04)	0.27 (0.05)	0.19 (0.02)	0.17 (0.01)
G_L cm^{-2} [µmol $CaCO_3$ h^{-1}]	1.55 (0.13)	1.85 (0.16)	4.31 (0.31)	1.83 (0.21)
G_L mg^{-1} biom. [µmol $CaCO_3$ h^{-1}]	0.78 (0.1)	0.64 (0.08)	1.19 (0.1)	0.44 (0.05)
G_D cm^{-2} [µmol $CaCO_3$ h^{-1}]	0.96 (0.1)	0.81 (0.1)	0.96 (0.11)	0.32 (0.12)
G_L/G_D	1.61 (0.12)	2.3 (0.13)	4.5 (0.21)	5.64 (0.16)
Zoox. density [no.*10^5 cm^{-2}]	5.25 (0.57)	9.16 (0.91)	6.58 (0.56)	7.13 (0.36)
Chl *a* cm^{-2} [µg]	3.56 (0.21)	7.47 (0.81)	12.09 (0.96)	17.87 (0.88)
Chl *a* zoox^{-1} [pg]	7.72 (1.13)	8.63 (0.84)	20.53 (2.11)	26.45 (1.36)
ZProt zoox^{-1} [ng]	0.67 (0.12)	0.33 (0.04)	0.73 (0.06)	0.4 (0.04)
TProt cm^{-2} [mg]	0.29 (0.03)	0.35 (0.05)	0.85 (0.11)	0.62 (0.04)
TProt mg^{-1} biom. [mg]	0.15 (0.02)	0.12 (0.02)	0.23 (0.03)	0.15 (0.01)
Biomass cm^{-2} [mg dry weight]	1.98 (0.18)	2.9 (0.27)	3.62 (0.15)	4.15 (0.13)